

## Supporting Information

# Boosted Photoelectrochemical Water Oxidation Performance with a Quaternary Heterostructure: CoFe<sub>2</sub>O<sub>4</sub>/MWCNT-Doped MIL-100(Fe)/TiO<sub>2</sub>

Waheed Rehman <sup>1</sup>, Faiq Saeed <sup>2</sup>, Yong Zhao <sup>3</sup>, Bushra Maryam <sup>1</sup>, Samia Arain <sup>4</sup>, Muhammad Ayaz <sup>5</sup>, Asad Jamil <sup>1</sup> and Xianhua Liu <sup>1,\*</sup>

- <sup>1</sup> School of Environmental Science and Engineering, Tianjin University, Tianjin 300072, China; waheedrehman@tju.edu.cn (W.R.); maryam\_bushra@tju.edu.cn (B.M.); asadjamil154@tju.edu.cn (A.J.)
- <sup>2</sup> Tianjin Key Laboratory of Molecular Optoelectronic Science, Department of Chemistry, School of Science, Tianjin University, Tianjin 300072, China; drfaiqsaeed@tju.edu.cn
- <sup>3</sup> 3rd Construction Co., Ltd. of China Construction 5th Engineering Bureau, Changsha 410021, China; cscec53@163.com
- <sup>4</sup> Tianjin Key Laboratory of Low-Dimensional Materials Physics and Preparing Technology, School of Science, Tianjin University, Tianjin 300072, China; samia@tju.edu.cn
- <sup>5</sup> School of Chemical Engineering and Technology, Tianjin University, Tianjin 300072, China; chemistazee@tju.edu.cn
- \* Correspondence: lxh@tju.edu.cn

## Figure and Table Captions

Figure S1. UV-vis absorbance spectra of CoFe<sub>2</sub>O<sub>4</sub>/MWCNTs@MIL-100(Fe)/TiO<sub>2</sub> and individual components.

Figure S2. XRD pattern of CoFe<sub>2</sub>O<sub>4</sub>/MWCNTs @ MIL-100 (Fe), CoFe<sub>2</sub>O<sub>4</sub>/MWCNTs, CoFe<sub>2</sub>O<sub>4</sub> samples with standard card JCPDS No.00-001-0646 and JCPDS No. 01-080-6487.

Figure S3. XRD pattern of CoFe<sub>2</sub>O<sub>4</sub>/MWCNTs@MIL-100(Fe)/TiO<sub>2</sub> sample before and after the reaction.

Figure S4. Raman spectrum of CoFe<sub>2</sub>O<sub>4</sub>.

Figure S5. Raman spectrum of CoFe<sub>2</sub>O<sub>4</sub>/MWCNTs.

Figure S6. Raman spectrum of CoFe<sub>2</sub>O<sub>4</sub>/MWCNTs doped MIL-100(Fe).

Table S1. Comparison of different pore size distribution of BET in CoFe<sub>2</sub>O<sub>4</sub>/MWCNT-doped MIL-100(Fe)/TiO<sub>2</sub>, CoFe<sub>2</sub>O<sub>4</sub>/MWCNTs doped MIL-100(Fe), CoFe<sub>2</sub>O<sub>4</sub>/MWCNTs and CoFe<sub>2</sub>O<sub>4</sub>.

Table S2. Photoelectrochemical parameters measured for the CoFe<sub>2</sub>O<sub>4</sub>/MWCNTs @MIL-100 (Fe) /TiO<sub>2</sub> photoanodes.

Table S3. Comparative analysis of performance of CoFe<sub>2</sub>O<sub>4</sub>/MWCNTs@MIL-100(Fe)/TiO<sub>2</sub> developed in this study against similar catalysts in photoelectrochemical (PEC) water splitting.

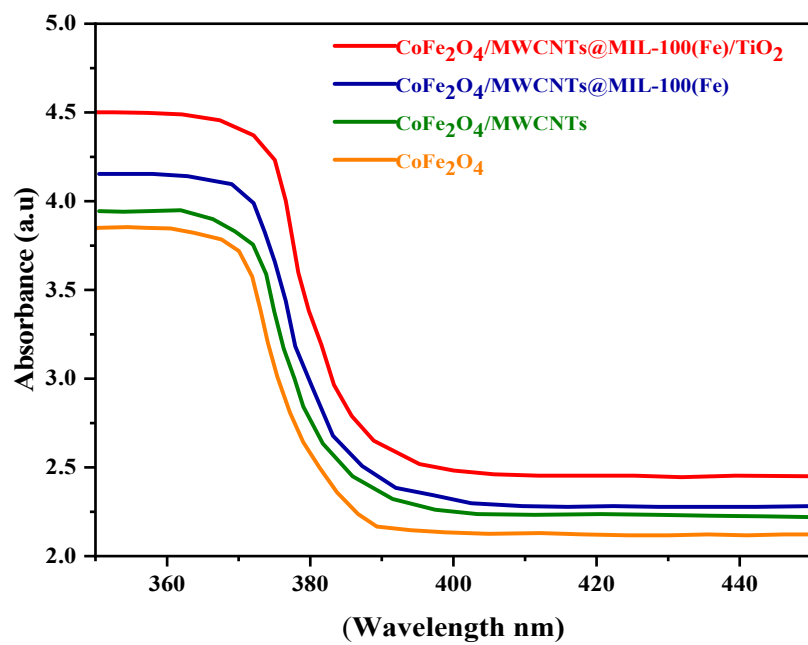


Figure S1. UV-vis absorbance spectra of CoFe<sub>2</sub>O<sub>4</sub>/MWCNTs@MIL-100(Fe)/TiO<sub>2</sub> and individual components.

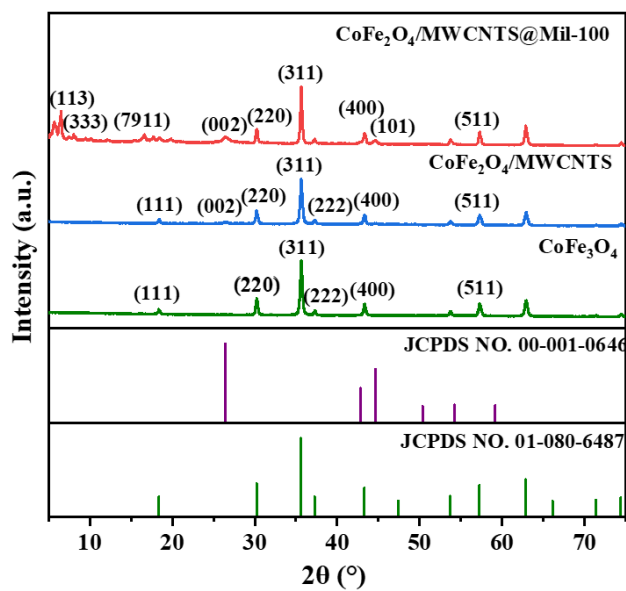


Figure S2. XRD pattern of  $\text{CoFe}_2\text{O}_4/\text{MWCNTs}@MIL-100$  (Fe),  $\text{CoFe}_2\text{O}_4/\text{MWCNTs}$ ,  $\text{CoFe}_3\text{O}_4$  samples with standard card JCPDS No.00-001-0646 and JCPDS No. 01-080-6487.

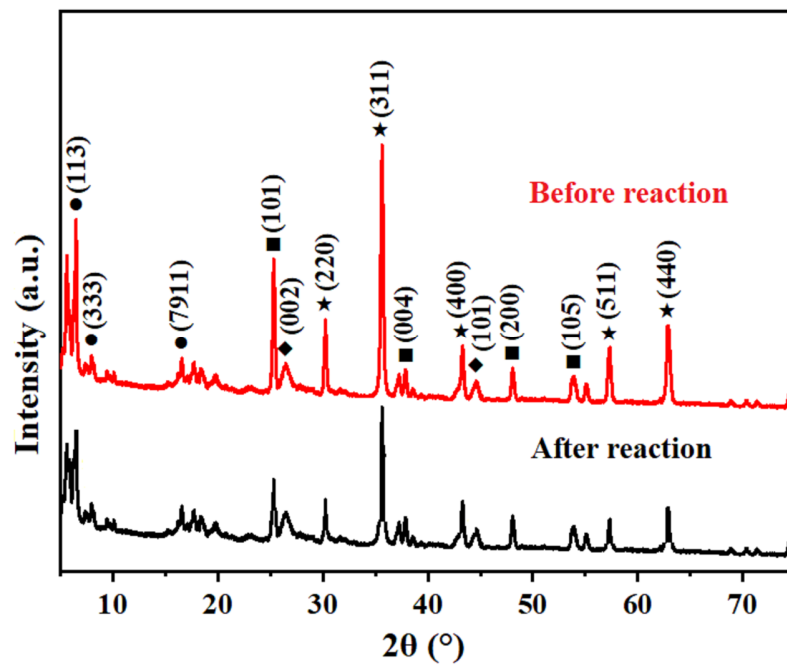


Figure S3. XRD pattern of samples before and after the reaction.

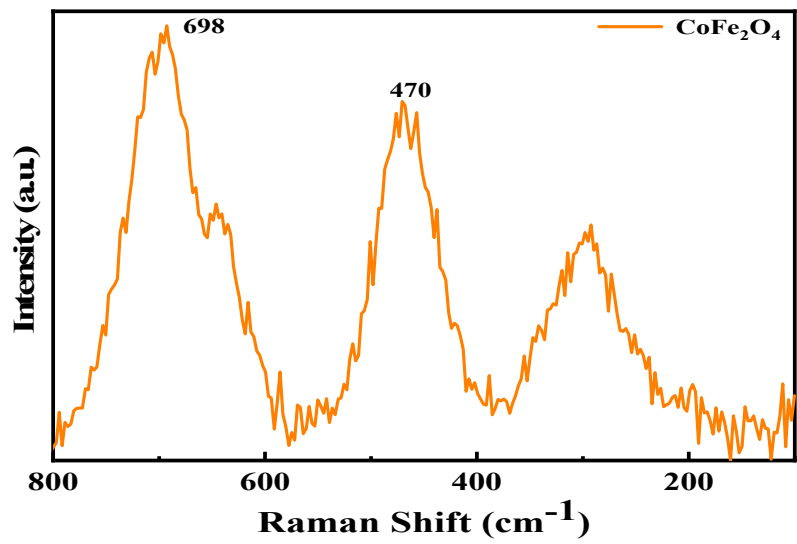


Figure S4. Raman spectrum of  $\text{CoFe}_2\text{O}_4$ .

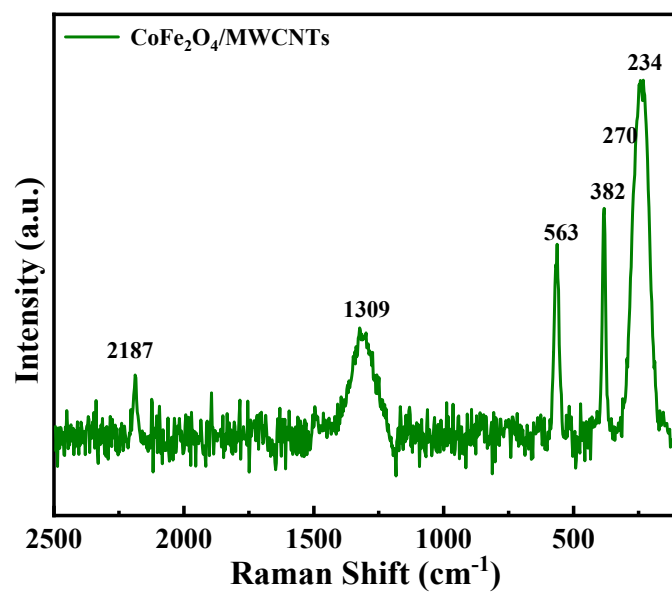


Figure S5. Raman spectrum of CoFe<sub>2</sub>O<sub>4</sub>/MWCNTs.

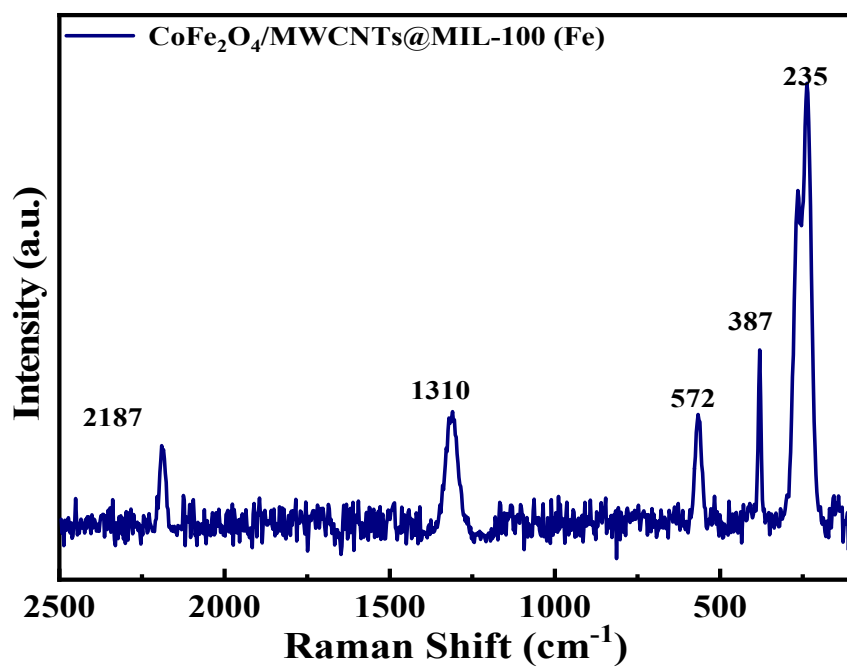


Figure S6. Raman spectrum of CoFe<sub>2</sub>O<sub>4</sub>/MWCNTs doped MIL-100(Fe).

Table S1. Comparison of different pore size distribution of BET in CoFe<sub>2</sub>O<sub>4</sub>/MWCNTs@MIL-100(Fe)/TiO<sub>2</sub>, CoFe<sub>2</sub>O<sub>4</sub>/MWCNTs doped MIL-100(Fe), CoFe<sub>2</sub>O<sub>4</sub>/MWCNTs and CoFe<sub>2</sub>O<sub>4</sub>.

<b>Sample</b>	<b>S<sub>BET</sub> (m<sup>2</sup> g<sup>-1</sup>)</b>	<b>Pore Volume (cm<sup>3</sup> g<sup>-1</sup>)</b>	<b>Average Pore Size (nm)</b>
<b>CoFe<sub>2</sub>O<sub>4</sub>/MWCNTs @MIL-100(Fe) /TiO<sub>2</sub></b>	1240	0.80 cm <sup>3</sup> /g.	18
<b>CoFe<sub>2</sub>O<sub>4</sub></b>	71	0.27	4
<b>MWCNTs</b>	260	0.13	15
<b>MIL-100(Fe)</b>	768.5	0.62	1.7
<b>TiO<sub>2</sub></b>	121	0.12	10

Table S2. Photoelectrochemical parameters measured for the CoFe<sub>2</sub>O<sub>4</sub>/MWCNTs @MIL-100 (Fe)/TiO<sub>2</sub> photoanodes.

<b>Catalyst</b>	<b><math>J_{ph}</math> (mA/cm<sup>2</sup>) at 1 V vs SCE</b>	<b><math>V_{oc}</math></b>	<b>Charge transfer resistance (Ohm)</b>	<b>ABPE (%)</b>	<b><math>V_{fb}</math></b>
CoFe <sub>2</sub> O <sub>4</sub>	0.16	0.26	55.31	0.07	-0.32
CoFe <sub>2</sub> O <sub>4</sub> /MWCNTs	1.92	0.39	26.97	1.19	-0.68
CoFe <sub>2</sub> O <sub>4</sub> /MWCNTs@ Mill-100(Fe)	5.17	0.67	23.62	4.60	-0.084
CoFe <sub>2</sub> O <sub>4</sub> /MWCNTs@ Mill-100(Fe)/TiO <sub>2</sub>	6.00	0.70	20.50	5.00	-0.09

Table S3. Comparative analysis of performance of CoFe<sub>2</sub>O<sub>4</sub>/MWCNTs@MIL-100(Fe)/TiO<sub>2</sub> developed in this study against similar catalysts in photoelectrochemical (PEC) water splitting.

<b>Catalyst Composition</b>	<b>Photocurrent Density (mA cm<sup>-2</sup>)</b>	<b>Applied Bias (V vs. RHE)</b>	<b>Incident Photon-to-Current Efficiency (IPCE) (%)</b>	<b>Stability</b>	<b>Reference</b>
TiO <sub>2</sub> /CoFe <sub>2</sub> O <sub>4</sub>	1.20	1.23	10 at 350 nm	Retained 85% over 10,000 s	[1]
TiO <sub>2</sub> /MWCNTs	2.20	1.23	12 at 350 nm	Retained 90% over 11,000 s	[2]
MIL-100(Fe)/TiO <sub>2</sub>	2.20	1.23	11 at 350 nm	Retained 92% over 12,000 s	[3]
TiO <sub>2</sub> (Pristine)	0.90	1.23	8 at 350 nm	Retained 80% over 8,000 s	[4]
Fe <sub>2</sub> O <sub>3</sub> /NiOOH	2.00	1.23	9 at 400 nm	Retained 85% over 15,000 s	[5]
Cu <sub>2</sub> O/TiO <sub>2</sub>	3.00	1.23	14 at 500 nm	Retained 90% over 10,000 s	[6]
ZnO/CdS	2.50	1.23	12 at 450 nm	Retained 88% over 12,000 s	[7]
g-C <sub>3</sub> N <sub>4</sub> /NiFe-LDH	3.20	1.23	13 at 420 nm	Retained 92% over 15,000 s	[8]

MoS <sub>2</sub> /TiO <sub>2</sub>	2.80	1.23	11 at 470 nm	Retained 87% over 10,000 s	[9]
CoFe <sub>2</sub> O <sub>4</sub> /MWCNTs@MI L-100(Fe)/TiO <sub>2</sub>	3.70	1.23	13 at 350 nm	Retained 95% over 12,000 s	This Work

#### REFERENCES:

1. Ibrahim, I.; Belessiotis, G.V.; Elseman, A.M.; et al. Magnetic TiO<sub>2</sub>/CoFe<sub>2</sub>O<sub>4</sub> photocatalysts for degradation of organic dyes and pharmaceuticals without oxidants. *Nanomaterials* **2022**, *12*, 3290.
2. Zeng, Q.; Li, H.; Duan, H.; et al. A green method to prepare TiO<sub>2</sub>/MWCNT nanocomposites with high photocatalytic activity and insights into the effect of heat treatment on photocatalytic activity. *RSC Advances* **2015**, *5*, 13430-13436.
3. Wang, T.; Liu, X.; Liu, M.; et al. The enhanced photocatalytic activity of TiO<sub>2</sub> (B)/MIL-100 (Fe) composite via Fe–O clusters. *New Journal of Chemistry* **2022**, *46*, 739-746.
4. Ziyilan-Yavas, A.; Mizukoshi, Y.; Maeda, Y.; et al. Supporting of pristine TiO<sub>2</sub> with noble metals to enhance the oxidation and mineralization of paracetamol by sonolysis and sonophotolysis. *Applied Catalysis B: Environmental* **2015**, *172*, 7-17.
5. Malara, F.; Minguzzi, A.; Marelli, M.; et al.  $\alpha$ -Fe<sub>2</sub>O<sub>3</sub>/NiOOH: an effective heterostructure for photoelectrochemical water oxidation. *ACS catalysis* **2015**, *5*, 5292-5300.
6. Wang, Y.; Zhang, Y.-n.; Zhao, G.; et al. Design of a novel Cu<sub>2</sub>O/TiO<sub>2</sub>/carbon aerogel electrode and its efficient electrosorption-assisted visible light photocatalytic degradation of 2, 4, 6-trichlorophenol. *ACS Applied Materials & Interfaces* **2012**, *4*, 3965-3972.
7. Abdel-Magied, A.F.; Abdelhamid, H.N.; Ashour, R.M.; et al. Magnetic metal-organic frameworks for efficient removal of cadmium (II), and lead (II) from aqueous solution. *Journal of Environmental Chemical Engineering* **2022**, *10*, 107467.
8. Nayak, S.; Mohapatra, L.; Parida, K. Visible light-driven novel gC<sub>3</sub>N<sub>4</sub>/NiFe-LDH composite photocatalyst with enhanced photocatalytic activity towards water oxidation and reduction reaction. *Journal of Materials Chemistry A* **2015**, *3*, 18622-18635.
9. Jia, P.-Y.; Guo, R.-t.; Pan, W.-g.; et al. The MoS<sub>2</sub>/TiO<sub>2</sub> heterojunction composites with enhanced activity for CO<sub>2</sub> photocatalytic reduction under visible light irradiation. *Colloids and Surfaces A: Physicochemical and Engineering Aspects* **2019**, *570*, 306-316.